Author Manuscript

Author Manuscript

Author Manuscript

Author Manuscript

HHS Public Access

Author manuscript

Cancer Biol Ther. Author manuscript; available in PMC 2015 November 24.

Published in final edited form as:

Cancer Biol Ther. 2008 November ; 7(11): 1774–1782.

Comedo-ductal carcinoma in situ:

A paradoxical role for programmed cell death

Malathy P.V. Shekhar[1,2,*], **Larry Tait**[1], **Robert J. Pauley**[1,2], **Gen Sheng Wu**[2,3], **Steven J. Santner**[1], **Pratima Nangia-Makker**[2,4], **Varun Shekhar**[5], **Hind Nassar**[2], **Daniel W. Visscher**[6], **Gloria H. Heppner**[1,7], and **Fred R. Miller**[1,2]

[1]Breast Cancer Program, Wayne State University, Detroit, Michigan USA

[2]Department of Pathology, Wayne State University, Detroit, Michigan USA

[3]Molecular Biology & Genetics Program, Wayne State University, Detroit, Michigan USA

[4]Protease Program, Karmanos Cancer Institute, Wayne State University, Detroit, Michigan USA

[5]Undergraduate Program, College of Liberal Arts and Sciences, Wayne State University, Detroit, Michigan USA

[6]Department of Pathology, University of Michigan, Ann Arbor, Michigan USA

[7]Department of Internal Medicine, Wayne State University, Detroit, Michigan USA

Abstract

Comedo-DCIS is a histologic subtype of preinvasive breast neoplasia that is characterized by prominent apoptotic cell death and has greater malignant potential than other DCIS subtypes. We investigated the mechanisms of apoptosis in comedo-DCIS and its role in conversion of comedo-DCIS to invasive cancer. Clinical comedo-DCIS excisions and the MCF10DCIS.com human breast cancer model which produces lesions resembling comedo-DCIS were analyzed. Apoptotic luminal and myoepithelial cells were identified by TUNEL and reactivity to cleaved PARP antibody and cell death assessed by Western blotting, Mitocapture and immunohistochemical assays. MCF10DCIS.com cells undergo spontaneous apoptosis in vitro, both in monolayers and multicellular spheroids; it is associated with increased mitochondrial membrane permeability, increase in Bax/Bcl-2 ratio and occurs via caspase-9-dependent p53-independent pathway. This suggests that apoptosis is stromal-independent and that the cells are programmed to undergo apoptosis. Immunostaining with cleaved PARP antibody showed that myoepithelial apoptosis occurs before lesions progress to comedo-DCIS in both clinical comedo-DCIS and in vivo MCF10DCIS.com lesions. Intense staining for MMP-2, MMP-3, MMP-9 and MMP-11 was observed in the stroma and epithelia of solid DCIS lesions prior to conversion to comedo-DCIS in clinical and MCF10DCIS.com lesions. Gelatin zymography showed higher MMP-2 levels in lysates and conditioned media of MCF10DCIS.com cells undergoing apoptosis. These data suggest that signals arising from the outside (microenvironmental) and inside (internal genetic alterations) of the duct act in concert to trigger apoptosis of myoepithelial and luminal epithelial cells. Our findings implicate spontaneous apoptosis in both the etiology and progression of

[*]Correspondence to: Malathy P.V. Shekhar; Breast Cancer Program; Karmanos Cancer Institute; 110 East Warren Avenue; Detroit, Michigan 48201 USA; shekharm@karmanos.org.

Author Manuscript Author Manuscript Author Manuscript Author Manuscript

comedo-DCIS. It is possible that spontaneous apoptosis facilitates elimination of cells thus permitting expansion and malignant transformation of cancer cells that are resistant to spontaneous apoptosis.

Keywords

spontaneous apoptosis; mitochondria; TUNEL; matrix metalloproteinases; gelatin zymography

Introduction

Breast ductal carcinoma in situ (DCIS) is histologically characterized by malignant-appearing cells confined to the ductal unit without evidence, by light microscopy, of invasion through the basement membrane into the surrounding stromal tissue. The introduction of high quality mammography has dramatically increased the detection rate of DCIS, as seen for women of all ethnic backgrounds and age groups.[1] In the U.S., age-adjusted incidence rates for DCIS increased from 2.4 per 100,000 women in 1973 to 15.8 per 100,000 women in 1992.[2] At present, 15–25% of all breast tumors diagnosed for women over 50 years of age are DCIS.[3] The natural history and biology of DCIS are poorly understood. Anecdotal evidence suggests that some breast cancers pass through a prolonged phase of DCIS prior to invasion whereas others progress more quickly from in situ to invasive disease and some may skip the preinvasive phase altogether.

DCIS represents a pathologically heterogeneous group of lesions with differing growth rates, a range of microarchitectural-cytological patterns and diverse malignant potentials. One clinically important histologic feature is the presence of intralumenal (comedo) necrosis. DCIS with comedo histology are most likely to recur following surgical excision and/or progress to invasive cancer.[4,5] In comparison to non-comedo-DCIS, comedo DCIS lesions are populated by larger and more pleomorphic neoplastic cells. They often demonstrate microinvasion,[6] and are characterized by greater chromosome aneuploidy,[7] higher proliferation rates[8] and more frequent Her2/neu gene amplification or protein overexpression[9] compared to non-comedo lesions.

The central necrosis in comedo-DCIS is of both apoptotic and oncotic types[10–12] although its natural history and contribution to disease pathogenesis is poorly understood. Mitochondria regulate cell death in response to growth factor withdrawal, DNA damage, hypoxia or oncogene deregulation and is critical for p53 dependent apoptosis.[13] When mitochondria receive a death signal, there is an increase in outer mitochondrial membrane permeability causing the release of apoptosis inducing factors and caspase activation.[13,14] Mitochondrial membrane integrity is regulated by opposing actions of pro- and anti-apoptotic Bcl-2 proteins that facilitate release of cytochrome *c* and other apoptogenic proteins from the intermembrane space of the mitochondria into the cytosol. The released cytochrome *c*, in the presence of dATP, binds to and activates adapter protein Apaf1 which in turn recruits and activates caspase-9 and subsequently executioner caspase-3, -6 or -7.[13] Besides cytoplasmic localization, pro- and active caspases-9 and -3 are localized in the mitochondria[15] (and references within). Pro-caspase-8, which is transcribed as two major

Author Manuscript Author Manuscript Author Manuscript Author Manuscript

isoforms, p55 and p53, was found to predominantly colocalize with the mitochondria in MCF-7 breast cancer cells.[16] There are no reports to date on the mechanisms of apoptosis in comedo-DCIS or the role of apoptosis in the conversion of comedo-DCIS to invasive cancer.

In the present study, we evaluated both clinically derived specimens of comedo-DCIS and MCF10DCIS.com cells. MCF10DCIS.com cells produce lesions resembling comedo-DCIS that uniformly progress to invasive cancer in immunodeficient nude mice.[17] The temporal progression of the in situ lesions to invasive cancer is reproducible.[18,19] Using a combination of staining with TUNEL and cleaved PARP (poly (ADP-ribose) polymerase) antibody, Western blot analysis and gelatin zymography of MCF10DCIS.com cells (monolayers, multicellular tumor spheroids, xenografts), or clinical comedo-DCIS, we show that “spontaneous” apoptosis plays an important role in both the etiology and progression of comedo-DCIS. The term “spontaneous” is used to describe the naturally occurring apoptosis in comedo-DCIS since it occurs in the absence of a nonphysiological stimulus and contrasts with the commonly studied “experimentally-induced” apoptosis.

Results

Conversion of MCF10DCIS.com xenografts to comedo-DCIS correlates with the initiation of apoptosis

Injection of MCF10DCIS.com cells into immunodeficient nude mice initially produces lesions resembling solid DCIS, in which ducts of malignant cells are surrounded by myoepithelial cells and an intact basement membrane;[17–19] (Fig. 1A, parts a and a′). As the lesions develop, cores of central comedo necrosis in duct lumens become initially detectable by ~30 days after injection, followed by pronounced comedo necrosis occupying the majority of the ducts after ~40 days (Fig. 1A, parts b and b′). The temporal progression of DCIS lesions produced by MCF10DCIS.com cells resemble the constellation of pathologic features observed in clinically-occurring clinical comedo-DCIS breast tumors (Fig. 1A, compare parts b, b′ with c–e) which are characterized by a mixture of ducts having lower grade nuclei and limited central necrosis (Fig. 1A, arrow in part c) and with ducts having higher grade nuclei and prominent lumenal necrosis (Fig. 1A, arrows in parts d and e).

Progression of solid DCIS into comedo-DCIS is initiated by naturally occurring apoptosis since detection of TUNEL-positive cells coincides with the appearance of central necrosis and is first observed in MCF10DCIS.com xenografts at ~30 days post injection (Fig. 1B, short arrows in part b). TUNEL-positive cells subsequently occupy the greater part of the xenograft ducts after 40 days post injection (Fig. 1B, part c).

Apoptosis in MCF10DCIS.com xenografts occurs independently of stroma

Since the conversion of MCF10DCIS.com xenografts from solid DCIS to comedo-DCIS lesions is characterized by the occurrence of spontaneous apoptosis, we tested whether initiation of apoptosis requires interaction with stromal components. Multicellular tumor spheroids were generated from MCF10DCIS.com cells on agarose and morphology of spheroids was examined by H&E staining of formalin-fixed paraffin embedded sections.

Author Manuscript Author Manuscript Author Manuscript Author Manuscript

Formation of multicellular spheroids was visible by day 2 (Fig. 2, part a) and by day 12, the majority of the spheroids, regardless of their size, showed the presence of necrotic centers (Fig. 2, parts b and c). This induction of cell death is likely not a result of nutrient deprivation, as spheroids generated by similar methods from MCF-7 (Fig. 2, part d) or MDA-MB-231 (data not shown) cells failed to produce necrotic centers. Furthermore, MCF10DCIS.com cells also underwent similar cell death in monolayer cultures (see below). Next, we performed TUNEL assays to determine whether cell death occurred via apoptosis. TUNEL-positive cells were observed in the central cores of MCF10DCIS.com-derived multicellular spheroids by day 6 (Fig. 2, compare parts e and f) and by day 12, pronounced central necrosis was observed in the spheroids (Fig. 2, part g) which resembled the day 44 comedo-DCIS lesions of MCF10DCIS.com xenografts (Fig. 1B, part c). No TUNEL positive cells were detected in spheroids generated from MCF-7 cells (Fig. 2, part h). TUNEL staining of MCF10DCIS.com monolayers revealed cells at varying stages of apoptosis and the percent of apoptotic cells ranged from 1–10% (Fig. 2, part i). These data suggest that MCF10DCIS.com cells are programmed to undergo apoptosis and that initiation of apoptotic triggers occurs independently of stromal microenvironment.

Spontaneous apoptosis of MCF10DCIS.com cells occurs via mitochondrial pathway

Since the results of Figure 2 demonstrated that multicellular spheroids and monolayers of MCF10DCIS.com cells undergo spontaneous apoptosis, we analyzed total cell lysates prepared from continuously passaged monolayers of MCF10DCIS.com cells at early, mid and late passages for steady-state levels of markers of apoptosis and compared them with parental MCF10A cells. Protein loading was monitored by staining with β-actin antibody. Consistent with our data from Figures 1B and 2, MCF10DCIS.com cells undergo apoptosis in monolayer cultures as ~2-, 4- and 10.5-fold higher levels of cleaved 17 kDa caspase-3 are detectable in MCF10DCIS.com cells at passages 13, 28 and 44, respectively, as compared to MCF10A cells (Fig. 3A). Western blot analysis of PARP showed that majority of PARP is cleaved to the 85 kDa fragment in MCF10DCIS.com cells (Fig. 3A), whereas approximately half of total PARP is present in its intact 115 kDa form in MCF10A cells (Fig. 3A). These data confirm that cleaved caspase-3 in MCF10DCIS.com cells is active. Western blot analysis of caspase-8 showed similar levels of p55 and p53 pro-caspase-8 forms in MCF10A and MCF10DCIS.com cells which remained uncleaved (Fig. 3A). In contrast, cleaved caspase-9 was detectable in early passage MCF10DCIS.com cells, which was further processed to p35 and/or 37 kDa forms in passages 28 and 44 cells whereas only the intact caspase-9 was detected in MCF10A cells (Fig. 3A). These data suggest that activation of caspase-3 in MCF10DCIS.com cells is mediated by caspase-9. Steady-state levels of Bcl-2 were downregulated ~8-fold in passage 28 and passage 44 MCF10DCIS.com cells as compared to passage 13 MCF10DCIS.com and MCF10A cells. Similar levels of Bax protein were detected in MCF10A and MCF10DCIS.com cells, however, the presence of ~18 kDa cleaved Bax fragment that is suggestive of proficient proapoptotic mitochondrial triggering was detected in MCF10DCIS.com cells (Fig. 3A). Consistent with these results, ~13–15-fold increase in Bax/Bcl-2 ratio was observed in passages 28 and 44 MCF10DCIS.com cells as compared to passage 13 MCF10DCIS.com and MCF10A cells (Fig. 3A). Spontaneous apoptosis of MCF10DCIS.com cells appears to occur by a p53-independent caspase-dependent pathway as progressive declines in p53 expression levels were observed in

Author Manuscript Author Manuscript Author Manuscript Author Manuscript

MCF10DCIS.com cells undergoing apoptosis (Fig. 3A). p53 protein levels were decreased by ~2 and 7.5-fold in passages 28 and 44 MCF10DCIS.com cells, respectively, as compared to passage 13 MCF10DCIS.com and MCF10A cells. Furthermore, despite abundant cell death, MCF10DCIS.com cells retained their proliferative potential as similar levels of PCNA expression were observed in passages 13, 28 and 44 MCF10DCIS.com and MCF10A cells (Fig. 3A).

The results of Western blot analysis were con- firmed by immunohistochemical staining of MCF10DCIS.com xenografts. Consistent with results from Western blot analysis, MCF10DCIS.com xenografts displayed intense reactivity to Bax antibody (Fig. 3B, part a), whereas Bcl-2 staining was weak (Fig. 3B, part b). Intense nuclear reactivity to p53 antibody was observed in a majority of cells comprising solid DCIS lesions (Fig. 3B, part c), whereas p53 staining, like Bcl-2 (data not shown) was diffuse and weak in MCF10DCIS.com xenografts displaying the comedo-DCIS phenotype (Fig. 3B, part d).

Since the results of Western blot analysis implicate mitochondria in cell death of MCF10DCIS.com cells, we monitored the integrity of mitochondrial membrane potential using the Mitocapture probe. This reagent aggregates in the mitochondria and produces red punctate mitochondrial fluorescence when the mitochondrial membrane potential is intact (negative with respect to cytoplasm). In apoptotic cells, Mitocapture cannot aggregate in the mitochondria due to altered membrane permeability and produces green diffuse cytoplasmic fluorescence. Punctate red fluoresce indicative of intact mitochondria was observed in ~98% of MCF10A (Fig. 3C, parts a and d) and ~85% of MCF10DCIS.com passage 13 (Fig. 3C, arrow in parts b and d) cells, whereas ~50% of passage 46 MCF10DCIS.com cells displayed diffuse green fluorescence (Fig. 3C, arrow in parts c and d). These results suggest that spontaneous cell death of MCF10DCIS.com cells is accompanied by loss of mitochondrial transmembrane potential. The presence of fragmented DNA in MCF10DCIS.com cells was verified by subjecting genomic DNA isolated from passage 44 MCF10DCIS.com cells to agarose gel electrophoresis. Whereas genomic DNA of parental MCF10A cells showed no evidence of fragmentation, fragmented DNA appeared as a trailing smear containing detectable bands at ~1300 and 600 bp in MCF10DCIS.com cells (Fig. 3C, part e).

Loss of myoepithelium is initiated by apoptosis

Disruption of the myoepithelial layer and basement membrane is a prerequisite for the conversion of DCIS to invasive carcinoma. We examined whether there is an association between the appearance of apoptosis-initiated comedo necrosis within the DCIS lesions and disruption of the myoepithelial layer. Paraffin embedded sections of MCF10DCIS.com xenografts and clinical comedo-DCIS breast tumors were stained with the TUNEL kit or antibody specific to cleaved PARP. The presence of a myoepithelial layer surrounding the comedo-DCIS lesions was verified by immunohistochemical staining with α-smooth muscle actin or p63 (marker for basal/progenitor cells of epithelial tissues) antibody. As shown in Figure 4A, MCF10DCIS.com xenografts displaying solid DCIS phenotype (prior to conversion to comedo-DCIS) lacked TUNEL-positive staining both at the periphery and in the interior of the ducts (Fig. 4A, part a). TUNEL-positive cells were detected on the periphery (Fig. 4A, part b, short arrow) of MCF10DCIS.com lesions that exhibited central

Author Manuscript Author Manuscript Author Manuscript Author Manuscript

TUNEL positivity (Fig. 4A, part b, long arrow), whereas MCF10DCIS.com xenografts displaying microinvasion (Fig. 4A, part c, short arrow) showed TUNEL-positive central cores (Fig. 4A, part c, long arrow) but lacked TUNEL-positive cells at the periphery (Fig. 4A, part c). Interestingly, immunostaining with antibody specific to cleaved PARP[20] revealed cleaved PARP-positive myoepithelial nuclei in solid DCIS (Fig. 4A, part d, short arrow and inset) as well as MCF10DCIS.com xenografts that progressed to comedo-type (Fig. 4A, part h, arrow). Immunohistochemical staining with p63 antibody (Fig. 4A, parts e and i) and α-smooth muscle actin (Fig. 4A, part f) confirmed the identity of cleaved PARP reactive myoepithelial layer. Dual staining with silver and α-smooth muscle actin antibody further validated the myoepithelial layer (Fig. 4A, part g, short arrows) juxtaposed to the silver-reactive basement membrane. MCF10DCIS.com xenografts that manifested pronounced central comedo necrosis showed focal loss of p63 staining (Fig. 4A, part i, arrows) and α-smooth muscle actin staining of the myoepithelium and breaks in the basement membrane (Fig. 4A, part k, arrows). Since several cleaved PARP- (Fig. 4A, part d, long arrow) and p63-positive cells juxtaposed to the myoepithelial layer were also observed in MCF10DCIS.com xenografts (Fig. 4A, parts e and i), suggest that apoptotic loss of myoepithelium and myoepithelial precursor cells with concomitant loss of basement membrane repair function may occur early in development of comedo-DCIS. Comedo-DCIS lesions with compromised myoepithelium showed amplification of p63-positive cells in regions of microinvasion (Fig. 4A, part j, arrow) suggesting that escape from apoptotic elimination of basal p63-positive stem/progenitor cells contribute to basal breast cancer.

The kinetics of myoepithelial loss in MCF10DCIS.com xenografts resembled clinical comedo-DCIS tumors. Normal breast tissues (Fig. 4B, part a) and solid DCIS tumors (data not shown) failed to show TUNEL staining of myoepithelial cells consistent with the presence of an intact p63-positive myoepithelial layer (Fig. 4B, part e) and collagen IV reactive basement membrane (data not shown). Focal to extensive loss of myoepithelial cells was observed in DCIS lesions displaying comedo-necrosis by TUNEL (Fig. 4B, parts b and f, short arrows), cleaved PARP (Fig. 4B, parts c and g, short arrows) and p63 (Fig. 4B, parts d and h, short arrows). Again, as in MCF10DCIS.com xenografts, cleaved PARP-positive myoepithelial nuclei were detected in clinical DCIS lesions before they progressed to comedo-DCIS.

Expression of matrix metalloproteinases (MMPs)

Since loss of myoepithelium is accompanied by breach of basement membrane as detected by collagen IV staining (Fig. 5A, part a), we examined the expression of collagenases MMP-2, MMP-9 and MMP-3 (stromelysin-1) and MMP-11 (stromelysin-3) in MCF0DCIS.com xenografts and clinical comedo-DCIS breast tumors. Expression of all MMPs was upregulated in periductal stromal and in epithelial compartments of MCF10DCIS.com xenografts (Fig. 5A, parts b–e) and clinical comedo-DCIS (Fig. 5B, parts a–e) whether or not comedo-necrosis is present. Gelatin zymography of total cell lysates and conditioned media of MCF10DCIS.com cells was performed at passages 13, 28 and 46 to identify the gelatinases, their activation status and secretion into the conditioned media. MMP-2 and MMP-9 were the most prominent gelatinases detected in the lysates of MCF10DCIS.com cells. Similar amounts of 92 kDa MMP-9 band were detected in the total

Author Manuscript Author Manuscript Author Manuscript Author Manuscript

cell lysates of MCF10DCIS.com cells at passages 13, 28 and 46. Lysates and conditioned media of late passage (passage 46) MCF10DCIS.com cells showed the presence of an ~66–72 kDa band which was enhanced ~3-fold in the conditioned media as compared to the corresponding cell lysates (Fig. 5A, part f). This band was not detectable in passage 13 MCF10DCIS.com lysates. The identity of the MMPs detected by gelatin zymography was further verified by Western blot analysis with MMP-2 and MMP-9 antibodies. Similar levels of pro-MMP-9 were detected in the lysates and conditioned media of passage 46 MCF10DCIS.com cells (Fig. 5A, part g). Western blot analysis of MMP-2 showed that passage 46 MCF10DCIS.com cells also expressed and secreted MMP-2 but unlike MMP-9, active or processed MMP-2 was detectable both in the conditioned media and cell lysates. Interestingly, the majority of the MMP-2 present inside the cells was present in the processed form (Fig. 5A, part g). These data suggest that MMP-2 originating from tumor cells may play an important role in comedo-DCIS pathogenesis of MCF10DCIS.com cells.

Discussion

Spontaneous apoptosis has been previously recognized in comedo-DCIS,[10–12] however, there are no reports on the mechanisms of apoptosis or its possible association with tumor progression (i.e., invasive growth). One reason for this is the unavailability of a suitable model system that is representative of clinical comedo-DCIS. Our data from the human MCF10DCIS.com xenograft model show that spontaneously dying MCF10DCIS.com cells present apoptotic features (e.g., loss of mitochondrial transmembrane potential, TUNEL-positivity and DNA fragmentation) that result in loss of epithelium from within the duct. The spontaneous cell death is mediated by activation of caspase-9 and caspase-3 and is independent of caspase-8. The noninvolvement of caspase-8 in apoptotic processing is not due to insufficient levels of caspase-8 as significant amounts of procaspase-8 p55 and p53 forms were detected in MCF10DCIS.com cells undergoing apoptosis. Our data from Western blot analysis of cell lysates prepared from MCF10DCIS.com monolayers are consistent with Mitocapture assays as an increase in mitochondrial membrane permeability of MCF10DCIS.com cells correlated with a dramatic drop in the Bcl-2/Bax ratio. A proapototic role for p53 at the mitochondria level has been proposed. Mihara et al.[21] demonstrated translocation of p53 to mitochondria in irradiated thymocytes which resulted in increased permeabilization of the outer mitochondrial membrane by forming complexes with antiapoptotic Bcl-X_L and Bcl-2 proteins and causing release of cytochrome *c*. It is interesting to note that spontaneous apoptosis of MCF10DCIS.com cells is associated with loss of p53 suggesting that mitochondrial permeabilization and downregulation of Bcl-2 occur independently of p53. Clinical comedo-DCIS, like MCF10DCIS.com cells, show a significant drop in Bcl-2 along with increase in mutant p53 levels.[22] The molecular nature of the apoptosis-initiating stimulus is not known at present; however, loss of Bcl-2 protein correlated with apoptosis induction in cultured cells (Fig. 3A) and xenografts (Fig. 3B). Since loss of Bcl-2 staining was observed in DCIS lesions showing early signs of apoptosis (Fig. 3B) and Bcl-2 protein remained downregulated in comedo-DCIS lesions with pronounced central comedo cores (data not shown), suggest that Bcl-2 protein degradation may serve as a potential initiating trigger for spontaneous apoptosis in comedo-DCIS. Both MCF10DCIS.com and clinical comedo-DCIS cell death occur naturally, rather than

Author Manuscript Author Manuscript Author Manuscript Author Manuscript

experimentally induced and hence may involve distinct molecules or pathways for induction of apoptotic process. It is interesting to note that despite abundant cell death, MCF10DCIS.com cells retain PCNA expression and suggest that cell sacrifice may enable selection of highly proliferative subpopulations with greater malignancy potential.

The central necrosis that is characteristic of comedo-DCIS has been presumed to occur because the central cells in a large duct are deprived of essential metabolites such as oxygen, possibly due to limited diffusion in the nonvascularized duct.[23] Our data from MCF10DCIS.com xenografts show that the initial appearance of TUNEL-positive cells in MCF10DCIS.com xenografts is also initiated in smaller ducts, suggesting that the induction of spontaneous cell death is not entirely due to mechanical forces such as elevated pressure in the ducts that results from elevated cell number or deprivation of vital nutrients. This notion is further corroborated by MCF10DCIS.com cells undergoing spontaneous cell death in vitro both in monolayers and multicellular tumor spheroids and suggest that these cells are programmed to undergo apoptosis and that stroma-derived factors are not required for the process. It is striking that widespread and near synchronous death occurs in comedo-DCIS breast tumors indicating an abrupt group behavior. These cells appear to die communally as if responding to an insult that triggers coordinated signals that disseminate throughout the entire duct.

Analyses of TUNEL-positive cells in clinical comedo-DCIS breast tumors and MCF10DCIS.com xenografts reveals a temporal link between the emergence of apoptotic luminal epithelial and myoepithelial cells within the ducts and in the periphery of ducts, respectively. Studies by Man et al.[24] have shown that the frequency of focal myoepithelial cell layer disruptions is independent of the size, length and architecture of the ducts,[25] suggesting that it is unlikely that myoepithelial loss is triggered by mechanical forces such as elevated pressure in the lumen due to increase in tumor cell number. These data further implicate the presence of coordinated or concerted mechanism(s) in progression/malignant conversion of comedo-DCIS. Of the various DCIS subtypes, DCIS of the comedo type confers the highest risk for progression to invasive carcinoma and/or recurrence.[4] Based on our findings, we propose that, compared with other DCIS subtypes, apoptotic cell losses in comedo-DCIS subtype may be a potential mechanism accounting for their increased proclivity of progressing to invasive cancer. It is possible that general elimination of cells by spontaneous apoptosis allows for selection and malignant transformation of apoptosis-resistant cancer cells. It is not known if the loss of myoepithelial and luminal epithelial populations in the comedo-DCIS lesions is triggered by a common insult or by distinct insult(s) acting on the exterior and interior of the ducts.

Although proteases are clearly important in invasion and metastasis of breast cancer, invasive breast cancer is defined by the loss of an intact basement membrane, not the presence of proteases. The myoepithelium functions to produce and maintain the basement membrane. Thus, loss of the myoepithelium is prerequisite to invasion. Upregulation of proteases may contribute to aberrant apoptosis by disrupting balance and control of intracellular proteolytic enzymes. Noncaspases including cathepsin, calpain, granzymes, proteosome, serine proteases,[26–29] and MMPs[30] have been implicated in apoptotic processing. The epithelium of DCIS tumors is physically separated from the stroma by both

Author Manuscript Author Manuscript Author Manuscript Author Manuscript

the myoepithelial cell layer and basement membrane and the degradation of the latter is essential for local invasion into the surrounding stroma. Degradation of basement membrane is attributed to the combined activities of proteolytic enzymes produced by the tumor cells and the surrounding stroma.[31] Proteases of the MMP family have been reported to be particularly important for peritumoral extracellular matrix lysis.[32,33] Immunohistochemical analysis of MMPs showed the presence of strong staining for gelatinases MMP-2 and MMP-9 and stromelysins-1 and -3 in the stromal and epithelial compartments of comedo-DCIS lesions. Gelatin zymography showed increases in levels of MMP-2 in cell lysates and conditioned media of MCF10DCIS.com cells undergoing spontaneous apoptosis, whereas similar levels of MMP-9 were detected in MCF10DCIS.com lysates and conditioned media regardless of their apoptotic status. These data suggest a potential role for MMP-2 in breakdown of the basement membrane and conversion of MCF10DCIS.com xenografts to invasive carcinoma. Expression of gelatinases alone does not result in loss of basement membrane since progression to intraductal carcinoma does not occur until both expression of gelatinases and loss of myoepithelium are apparent. Further, gelatinase-induced disruption of basement membrane may be repaired by a functionally intact myoepithelial layer. Lymphocytic infiltration has been reported as potential source of protease production and has been implicated to play an important role in loss of the myoepithelial layer.[34] Although influences from these stromal components may play an active role in myoepithelial loss and malignant conversion of comedo-DCIS, immunostaining of clinical comedo-DCIS breast tumors showed intense staining for MMP-2, -9, -3 and -11 in solid DCIS lesions (prior to becoming comedo-DCIS), much before the loss of the myoepithelial cell layer, with continued increase in high grade comedo-DCIS lesions showing myoepithelial loss and basement membrane degradation. These data suggest that tumor cells may generate the initiating signals (proteases?) and that lymphocytic reactions frequently observed in high grade DCIS (Fig. 5B, part e) may reinforce the protease production and enable selection of aggressive tumor subpopulations.[35] This notion is consistent with our results from in vitro assays that showed that MCF10DCIS.com cells themselves provide the impetus for the apoptotic process although the precise nature of the trigger for apoptosis remains to be determined.

In summary, our results from the human MCF10DCIS.com xenograft model and clinical comedo-DCIS breast tumors have revealed novel insights into the biology and mechanism of malignant conversion of comedo-DCIS and emergence of basal breast cancer and implicate spontaneous cell death, generally considered a favorable feature, in both the etiology and progression of comedo-DCIS.

Materials and Methods

Cell culture

MCF10DCIS.com cells were maintained in DMEM/F12 medium (1:1) supplemented with 5% horse serum and 4 mM glutamine.[17,18] Cells were maintained in a 37°C humidified incubator with an atmosphere of 5% CO_2. Single-cell suspensions were prepared by treatment with trypsin-EDTA (Life Technologies, Inc., Carlsbad, CA) and resuspended in complete medium before setting up monolayer or multicellular tumor spheroid cultures. For

Author Manuscript Author Manuscript Author Manuscript Author Manuscript

experimental evaluation of temporal changes in apoptotic processes in monolayer, cells were continuously grown from passages 13 to 46. Cells are normally kept frozen in liquid nitrogen. Cells are recovered from liquid nitrogen and expanded for 3–5 passes prior to use in xenografts or growth as spheroids.

Generation of MCF10DCIS.com xenografts and multicellular tumor spheroids

Xenograft tumors were generated by injecting 1×10^6 cells in 0.1 ml Matrigel subcutaneously near the nipple of gland #5 of female nude mice.[18] Xenografts were removed at various periods of growth and fixed in buffered formalin. Multicellular tumor spheroids were generated using the liquid overlay technique. Briefly, six well culture plates were coated with 2 ml of 1% Seaplaque agarose (FMC Bioproducts, Rockland, ME). Cells (1×10^6) from a single-cell suspension were added per well in a total volume of 2 ml of DMEM/F-12 growth medium. Spheroids were allowed to form over 48 hours and maintained up to 6–10 days for analysis of morphology and spontaneous apoptosis. Spheroids were allowed to settle, rinsed with phosphate buffered saline and fixed in 10% buffered formalin.

Immunohistochemistry

Non-identifiable comedo-DCIS breast tumors were acquired after protocol review and approval by the Wayne State University Human Investigation Committee. Four micron sections from formalin-fixed, paraffin embedded clinical comedo-DCIS, MCF10DCIS.com xenografts and MCF10DCIS.com-derived multicellular tumor spheroids were stained with hematoxylin and eosin (H&E) for morphological analysis, or incubated with primary antibodies followed by appropriate biotinylated secondary antibody and HRP-conjugated streptavidin, or FITC-conjugated secondary antibody. Nuclei were counterstained with hematoxylin or DAPI. Control sections were stained with corresponding normal IgG or secondary antibody only. The following primary antibodies were used: p53 DO-7 (Dako, Carpinteria, CA), Bcl-2 (Santa Cruz Biotechnology, Inc., Santa Cruz, CA), Bax (Santa Cruz), cleaved PARP (Cell Signaling Technology, Inc., Danvers, MA), p63 (Santa Cruz), α-smooth muscle actin (Dako), MMP-3 (Oncogene Science, Cambridge, MA), MMP-9 (Oncogene Science), MMP-2 (Oncogene Science), MMP-11 (Oncogene Science) and type IV collagen (Dako). The presence of basement membrane was demonstrated by staining with silver methamine-borate (Sigma Diagnostics) as described previously.[36] In some cases, sections were dual stained with α-smooth muscle actin antibody and silver stain for localization of myoepithelium and basement membrane.

Terminal deoxynucleotidyl transferase biotin-dUTP nick end-labeling

Apoptotic cells in clinical comedo-DCIS breast tumors, comedo-DCIS lesions of MCF10DCIS.com xenografts and MCF10DCIS.com multicellular tumor spheroids were identified on deparaffinized sections using the Deadend fluorimetric TUNEL system (Promega Corp., Madison, WI). Sections were counter-stained with propidium iodide and cells within the central comedo cores and myoepithelial layer with yellow or green nuclear staining were scored as apoptotic cells. For identification of apoptotic cells in MCF10DCIS.com monolayers, cells were cultured on 8-well chamber slides, fixed in phosphate-buffered formalin and permeabilized with 0.2% Triton X-100 prior to TUNEL

Author Manuscript Author Manuscript Author Manuscript Author Manuscript

staining. Images were captured with an Olympus BX40 microscope and processed with the M5$^+$ microcomputer imaging device (Interfocus Imaging, Ltd., Cambridge, U.K.).

Mitochondria mediated cell death

Cell death was assessed according to the supplier's instructions by staining MCF10DCIS.com or parental control MCF10A cells with Mitocapture (BioVision, Mountain view, CA), a fluorescent lipophilic cationic reagent that assesses mitochondrial membrane permeability. MCF10DCIS.com cells that were continuously passaged for the indicated number of passages were used. Briefly, cells were incubated with the MitoCapture reagent for 15 min at 37°C and visualized by fluorescence microscopy using a wide band pass filter (detects FITC and rhodamine). All images were collected on an Olympus BX-40 fluorescence microscope equipped with Sony high resolution/sensitivity CCD video camera. Cells with intact mitochondria exhibit punctuate red cytosolic fluorescence, whereas cells with permeabilized mitochondria exhibit diffuse green cytosolic fluorescence. The numbers of cells showing red fluorescence or diffuse green fluorescence were scored by counting three-five fields of ~100 cells each. Each experiment was repeated at least three times and results expressed as mean ± S.E. Statistical significance of differences was determined by Student's t test.

Western blot analysis

Whole cell lysates were prepared from MCF10DCIS.com monolayers that were continuously passaged for ~10–15 (early), ~25–30 (mid), or ~42–50 (late) passages as described previously.[37] Protein concentration was evaluated using the Bio-Rad (Hercules, CA) protein assay. Samples containing 25 μg total protein were separated by SDS-PAGE and transferred to polyvinylidene difluoride membranes. Membranes were probed with the following antibodies: Bcl-2 (Santa Cruz), Bax (Santa Cruz), p53 pAb421 (Oncogene Science), PCNA (Dako), caspases-9, -8, -3 (Oncogene Science) and PARP (clone C-2-10; Invitrogen Corporation, Carlsbad, CA). Steady-state levels of pro- and processed forms of MMP-2 and -9 in total cell lysates or conditioned media of MCF10DCIS.com cells undergoing apoptosis were detected by immunoblotting with anti-MMP-2 or MMP-9 antibodies. Protein loading was monitored by reprobing the stripped membranes with β-actin antibody (Sigma Chemicals, St. Louis, MO). Detection was performed with enhanced chemiluminescence kit (Amersham, Piscataway, NJ) and exposure to X-ray film. The amounts of markers relative to β-actin were quantitated with NIH Imaging software.

Gelatin zymography

The activity of gelatinolytic enzymes in the conditioned media and total cell lysates of MCF10DCIS.com cells that were continuously passaged for ~13, 28 or 46 passages was detected by electrophoresis on 7.5% polyacrylamide gels containing gelatin at a final concentration of 0.6 mg/ml. Samples containing equivalent amounts of total protein (50 μg) were mixed with SDS sample buffer and electrophoresed under nonreducing conditions.[38] After electrophoresis, gels were soaked for 10 minutes in 2.5% Triton X-100/10 mM Tris-HCl (pH 8.0) at room temperature, rinsed and incubated at 37°C for 16 hours in 5 mM $CaCl_2$/50 mM Tris-HCl (pH 8). Gels were stained with 0.1% Coomassie Brilliant Blue R250 and destained.

Author Manuscript Author Manuscript Author Manuscript Author Manuscript

Acknowledgments

Supported by U.S. Army Medical Research and Materiel Command DAMD17-02-1-0618 (MPS), Karmanos Cancer Institute Strategic Research Initiative grant (MPS, FRM) and National Institutes of Environmental Health Sciences P30 E506639 Environmental Health Sciences Center Grant.

Abbreviations

DCIS	ductal carcinoma in situ
MMP	matrix metalloproteinase
TUNEL	terminal deoxynucleotidyl transferase biotin-dUTP nick end-labeling
PARP	poly (ADP-ribose) polymerase

References

1. Ernster V, Barclay J, Kerlikowske K, Grady D, Henderson C. Incidence of and treatment for ductal carcinoma in situ of the breast. J Am Med Assoc. 1996; 275:913–8.
2. Leonard GD, Swain SM. Ductal carcinoma in situ, complexities and challenges. J Natl Cancer Inst. 2004; 96:906–20. [PubMed: 15199110]
3. Jemal A, Siegel R, Ward E, Murray T, Xu J, Thun MJ. Cancer statistics, 2007. CA Cancer J Clin. 2007; 57:43–66. [PubMed: 17237035]
4. Fisher ER, Land SR, Saad RS, Fisher B, Wickerham DL, Wang M, et al. Pathologic variables predictive of breast events in patients with ductal carcinoma in situ. Am J Clin Pathol. 2007; 128:86–91. [PubMed: 17580274]
5. Yang M, Moriya T, Oguma M, Cruz CDL, Endoh M, Ishida T, et al. Microinvasive ductal carcinoma (T1mic) of the breast. The clinicopathological profile and immunohistochemical features of 28 cases. Pathol Int. 2003; 53:422–8. [PubMed: 12828606]
6. Jaffer S, Bleiweiss IJ. Histologic classification of ductal carcinoma in situ. Microscopy Res & Techniques. 2002; 59:92–101.
7. Aasmundstad T, Haugen O. DNA ploidy in intraductal breast carcinomas. Eur J Cancer. 1992; 26:956–9. [PubMed: 2177615]
8. Meyer J. Cell kinetics of histologic variants of in situ breast carcinoma. Breast Cancer Res Treat. 1986; 7:171–80. [PubMed: 3022849]
9. Van de Vijver MJ, Peterse JL, Mooi WJ, Wisman P, Lomans J, Dalesio O, et al. Neu-protein overexpression in breast cancer: Association with comedo-type ductal carcinoma in situ and limited prognostic value in stage 2 breast cancer. New Engl J Med. 1988; 319:1239–45. [PubMed: 2903446]
10. Gandhi A, Holland PA, Knox WF, Potten CS, Bundred NJ. Evidence of significant apoptosis in poorly differentiated ductal carcinoma in situ of the breast. Br J Cancer. 1988; 78:788–94. [PubMed: 9743302]
11. Moinfar F, Mannion C, Man YG, Tavassoli FA. Mammary “comedo”-DCIS: apoptosis, oncosis and necrosis: an electron microscopic examination of 8 cases. Ultrastruct Pathol. 2000; 24:135–44. [PubMed: 10914424]
12. Bodis S, Siziopikou KP, Schnitt SJ, Harris JR, Fisher DE. Extensive apoptosis in ductal carcinoma in situ of the breast. Cancer. 1996; 77:1831–5. [PubMed: 8646681]
13. Wang X. The expanding role of mitochondria in apoptosis. Genes Dev. 2001; 15:2922–33. [PubMed: 11711427]
14. Ravagnan L, Rouimer T, Kroemer G. Mitochondria, the killer organelles and their weapons. J Cell Physiol. 2002; 192:131–7. [PubMed: 12115719]
15. Chandra D, Tang DG. Mitochondrially located active caspase-9 and caspase-3 result mostly from translocation from the cytosol and partly from caspase-mediated activation in the organelle. Lack

Author Manuscript Author Manuscript Author Manuscript Author Manuscript

of evidence for Apaf-1-mediated procaspase-9 activation in the mitochondria. J Biol Chem. 2003; 278:17408–20. [PubMed: 12611882]

16. Stegh AH, Barnhart BC, Volkland J, Algeciras-Schimnich A, Ke N, Reed JC, et al. Inactivation of caspase-8 on mitochondria of Bcl-x_L-expressing MCF7-Fas cells: Role for the bifunctional apoptosis regulator protein. J Biol Chem. 2002; 277:4351–60. [PubMed: 11733517]
17. Miller FR, Santner SJ, Tait L, Dawson PJ. MCF10DCIS. com xenograft model of human comedo ductal carcinoma in situ. J Nat Cancer Inst. 2000; 92:1185–6. [PubMed: 10904098]
18. Tait LR, Pauley RJ, Santner SJ, Heppner GH, Heng HH, Rak JW, et al. Dynamic stromal-epithelial interactions during progression of MCF10DCIS. com xenografts. Int J Cancer. 2007; 120:2127–34. [PubMed: 17266026]
19. Hu M, Yao J, Carroll DK, Weremowicz S, Chen H, Carrasco D, et al. Regulation of in situ to invasive breast carcinoma transition. Cancer Cell. 2008; 13:394–406. [PubMed: 18455123]
20. Oliver FJ, de la Rubia G, Rolli V, Ruiz-Ruiz MC, de Murcia G, Murcia JM. Importance of poly(ADP-ribose) polymerase and its cleavage in apoptosis. Lesson from an uncleavable mutant. J Biol Chem. 1998; 273:33533–9. [PubMed: 9837934]
21. Mihara M, Erster S, Zaika A, Petrenko O, Chittenden T, Pancoska P, et al. p53 has a direct apoptogenic role at the mitochondria. Mol Cell. 2003; 11:577–90. [PubMed: 12667443]
22. Megha T, Ferrari F, Arcuri F, Lalinga AV, Lazzi S, Cardone C, et al. Cellular kinetics and expression of bcl-2 and p53 in ductal carcinoma of the breast. Oncol Rep. 2000; 7:473–8. [PubMed: 10767354]
23. Franks SJ, Byrne HM, Underwood JCE, Lewis CE. Biological inferences from a mathematical model of comedo ductal carcinoma in situ of the breast. J Theoret Biol. 2005; 232:523–43. [PubMed: 15588633]
24. Man YG, San QX. The significance of focal myoepithelial cell layer disruptions in human breast tumor invasion: A paradigm shift from the “protease-centered” hypothesis. Exp Cell Res. 2004; 301:103–18. [PubMed: 15530847]
25. Man YG, Tai L, Barner R, Vang R, Saenger JS, Shekitka KM, et al. Cell clusters overlying focally disrupted mammary myoepithelial cell layers and adjacent cells within the same duct display different immunohistochemical and genetic features: Implications for tumor progression and invasion. Breast Cancer Res. 2003; 5:231–41.
26. Solary E, Evmin B, Droin N, Haugg M. Proteases, proteolysis and apoptosis. Cell Biol Toxicol. 1988; 14:121–32. [PubMed: 9553723]
27. Kidd VJ, Lahti JM, Teitz T. Proteolytic regulation of apoptosis. Sem Cell Dev Biol. 2000; 11:191–201.
28. Johnson DE. Noncaspase proteases in apoptosis. Leukemia. 2000; 14:1695–703. [PubMed: 10995018]
29. Egger L, Schneider J, Rhemec C, Tapernoux M, Hacki J, Borner C. Serine proteases mediate apoptosis-like cell death and phagocytosis under caspase-inhibiting conditions. Cell Death Differ. 2003; 10:1188–203. [PubMed: 14502242]
30. Sutherland KD, Lindeman GJ, Vsvader JE. The molecular culprits underlying precocious mammary gland involution. J Mammary Gland Biol Neoplasia. 2007; 12:15–23. [PubMed: 17323120]
31. Rudolph-Owen LA, Matrisian LM. Matrix metalloproteinases in remodeling of the normal and neoplastic mammary glands. J Mammary Gland Biol Neoplasia. 1998; 3:177–89. [PubMed: 10819526]
32. Stamenkovic I. Matrix metalloproteinases in tumor invasion and metastasis. Semin Cancer Biol. 2000; 10:415–33. [PubMed: 11170864]
33. Brinckerhoff CE, Rutter JL, Benbow U. Interstitial collagenases as markers of tumor progression. Clin Cancer Res. 2000; 6:4823–30. [PubMed: 11156241]
34. Yousefi M, Mattu R, Gao C, Man YG. Mammary ducts with and without focal myoepithelial cell layer disruptions show a different frequency of white blood cell infiltration and growth pattern: Implications for tumor progression and invasion. Appl Immunohistochem Mol Morphol. 2005; 13:30–7. [PubMed: 15722791]

Author Manuscript Author Manuscript Author Manuscript Author Manuscript

35. Smith HS, Lu Y, Deng G, Martinez O, Krams S, Ljung BM, et al. Molecular aspects of early stages of breast cancer progression. J Cell Biochem Suppl. 1993; 17:144–52. [PubMed: 8007693]

36. Tait L, Dawson PJ, Wolman SR, Galea K, Miller FR. Multipotent human breast stem cell line MCF10AT. Int J Oncol. 1996; 9:263–7. [PubMed: 21541510]

37. Shekhar MP, Lyakhovich A, Visscher DW, Heng H, Kondrat N. Rad6 overexpression induces multinucleation, centrosome amplification, abnormal mitosis, aneuploidy and transformation. Cancer Res. 2002; 62:2115–24. [PubMed: 11929833]

38. Shekhar MP, Werdell J, Tait L. Interaction with endothelial cells is a prerequisite for branching ductal-alveolar morphogenesis and hyperplasia of preneoplastic human breast epithelial cell: Regulation by estrogen. Cancer Res. 2000; 60:439–49. [PubMed: 10667599]

Author Manuscript Author Manuscript Author Manuscript Author Manuscript

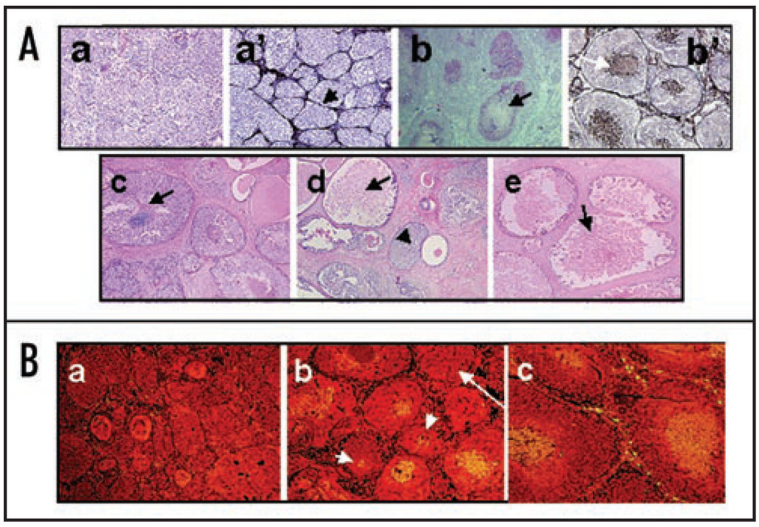

Figure 1.

(A) Comparative morphologies of clinical comedo-DCIS (c–e) and MCF10DCIS.com xenografts (a, a′, b, b′). Panels (a and b), H&E of MCF10DCIS.com xenografts at days 20 and 44, respectively. Panels (a′ and b′), silver staining of MCF10DCIS.com xenografts at days 20 and 44, respectively. Panels (c–e), H&E of clinical comedo-DCIS breast tumors. Note that MCF10DCIS.com xenografts initially organize into solid DCIS lesions surrounded by basement membrane (arrow in a′) before conversion to comedo-DCIS. Arrows in (b, b′ and c–e), indicate necrotic cores and the arrowhead in (d), solid DCIS. Original magnification x10. (B) MCF10DCIS.com xenografts undergo spontaneous apoptosis. Panels (a–c), TUNEL staining for xenografts harvested at days 20, 30 and 44 days, respectively. Note the presence of central TUNEL-positive cells in (b and c) and its absence in (a). Also, note that TUNEL positivity is not related to the size of the ducts as some small ducts are TUNEL positive (short arrows in b), whereas some larger ducts (long arrow in b) are TUNEL-negative. Original magnification x10.

Author Manuscript Author Manuscript Author Manuscript Author Manuscript

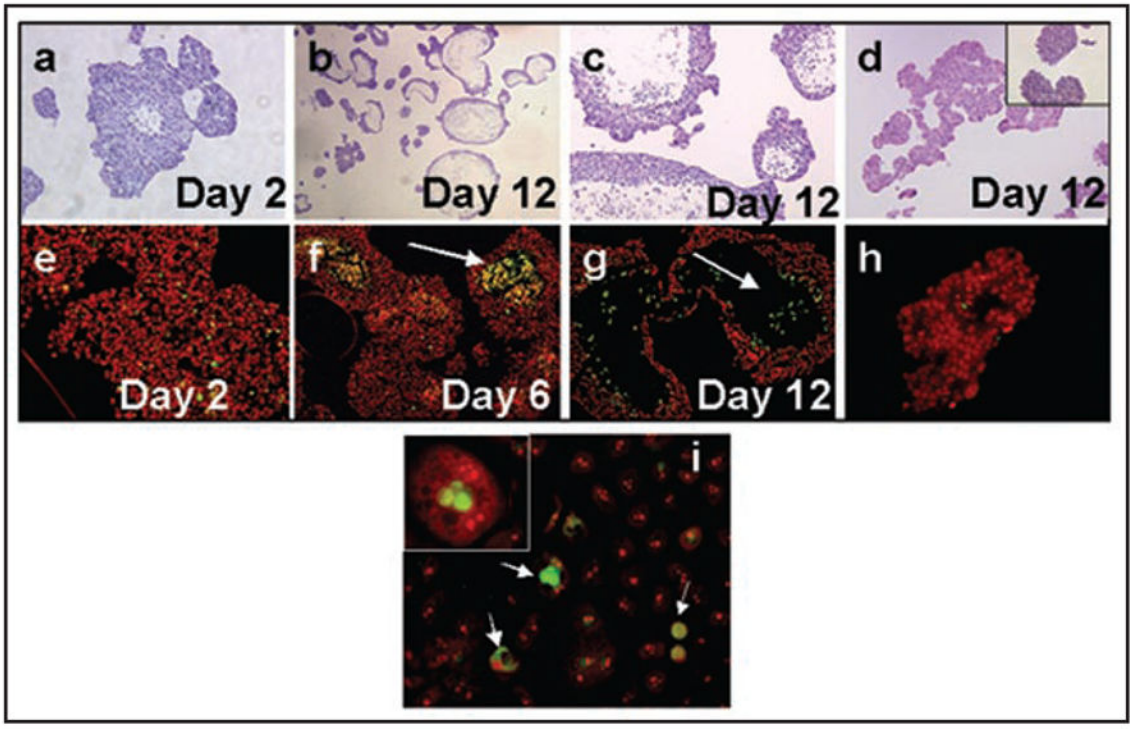

Figure 2.

Multicellular spheroids of MCF10DCIS.com cells undergo spontaneous apoptosis. Panels (a–c) and (e–g), MCF10DCIS.com derived spheroids; panels (d and h), multicellular spheroids generated from MCF-7 breast cancer cells; panel (i), MCF10DCIS.com monolayer. Panels (a–d), H&E staining and (e–i), TUNEL staining. Note the presence of TUNEL-positive cells within the MCF10DCIS.com spheroids (arrows in f and g) and monlayers (arrows in i) and their absence in MCF-7 derived spheroids (h) and MCF10DCIS.com spheroids at day 2 (e). The insets in (d and i) are higher magnifications of MCF-7 spheroids and TUNEL-positive MCF10DCIS.com cells, respectively. Original magnification x4 (b); X10 (a, c–g, i); x20 (h and inset in d); x100 (inset in i).

Author Manuscript Author Manuscript Author Manuscript Author Manuscript

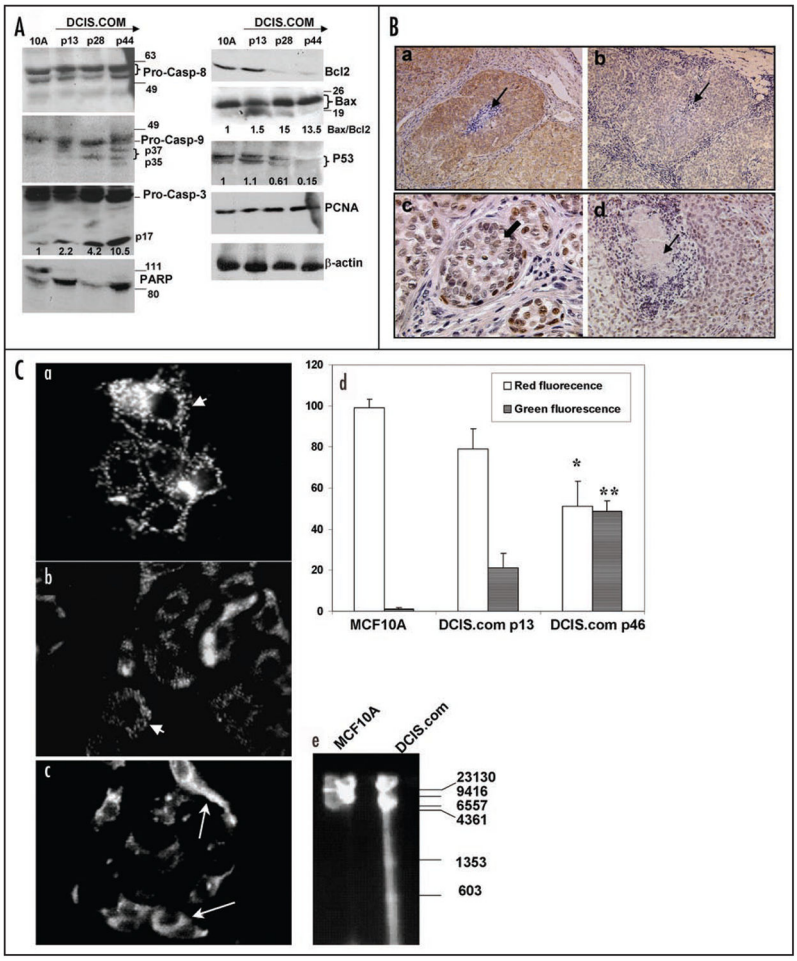

Figure 3.

Spontaneous apoptosis of MCF10DCIS.com cells is associated with caspase-9 activation and downregulation of Bcl-2 and p53. (A) Whole cell lysates prepared from monolayers of MCF10A, or MCF10DCIS.com cells continuously passaged for 13 (early), 28 (mid) and 44 (late) passages were analyzed by Western blotting for the indicated markers. Levels of activated 17 kDa caspase-3, p53 and Bax to Bcl-2 ratios relative to β-actin loading control are indicated. (B) Immunohistochemical analysis of Bax (a), Bcl-2 (b) and p53 (c and d) in MCF10DCIS.com xenografts. Thin arrows in (a, b and d), indicate comedo cores and the thick block arrow in (c) indicates p53 reactivity in day 12 MCF10DCIS.com solid DCIS lesions. Original magnification X10 (a and b); X40 (c); X20 (d). (C) A typical labeling pattern of MCF10A (a), or MCF10DCIS.com cells continuously passed for 13 (b) or 46 (c) passages with Mitocapture reagent is shown. Short arrows in (a and b) show cells containing punctuate red fluorescence and long arrows in (c) indicate cells with diffuse green cytoplasm. (d) Graphic representation of percent of cells exhibiting punctuate red fluorescence or diffuse green cytoplasm. Values are mean ± S.E. * and **, indicate significant differences in percent of cells containing punctuate red fluorescence or diffuse green cytoplasm between MCF10DCIS.com cells at passages 13 and 46, respectively ($p < 0.001$). (e) Agarose gel electrophoresis of genomic DNA isolated from MCF10A or MCF10DCIS.com passage 46 cells.

Author Manuscript Author Manuscript Author Manuscript Author Manuscript

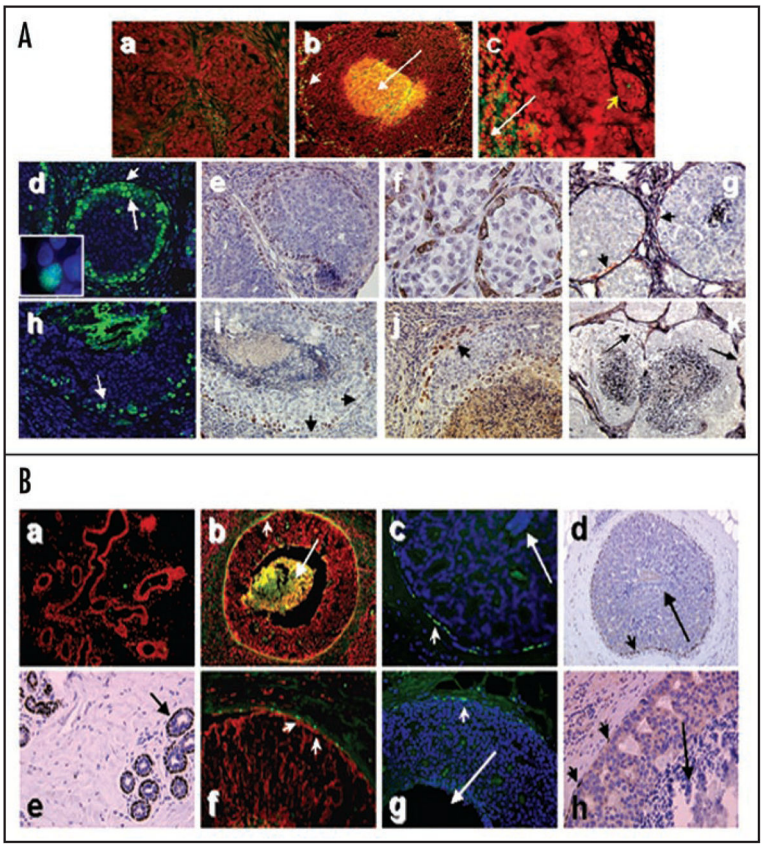

Figure 4.

Association between apoptotic loss of luminal epithelial and myoepithelial cells in comedo-DCIS. (A) TUNEL (a–c), cleaved PARP (d and h), p63 (e, i and j) and α-smooth muscle actin (f, g and k) staining of MCF10DCIS.com xenografts. Panels (a, d, e and f) are MCF10DCIS.com lesions at 22 days; panel g, 30 days; panels (b, h, i and j), 44 days; panel (c and k), 55 days. Panels (g and k), Dual staining with silver and α-smooth muscle actin. Note the presence of α-smooth muscle actin-positive myoepithelial cells (pink color) juxtaposed to the basement membrane in g (arrows) and absence in i. Arrows in k indicate basement membrane loss. Original magnification, x10 (b and k); x20 (a, d, e, g–i and j); x40 (c and f). (B) TUNEL (a, b and f), cleaved PARP (c and g) and p63 (d, e and h) staining of breast tissues. Panels (a and e), normal ducts; (b–d and f–h), comedo-DCIS breast tumors. Long arrows in (b–d, g and h), indicate comedo cores. Short arrows in (b–d and f–h) indicate reactive myoepithelial cells. Original magnification, x10 (a, b and d); x20 (c, e, f and g); x40 (h).

Author Manuscript Author Manuscript Author Manuscript Author Manuscript

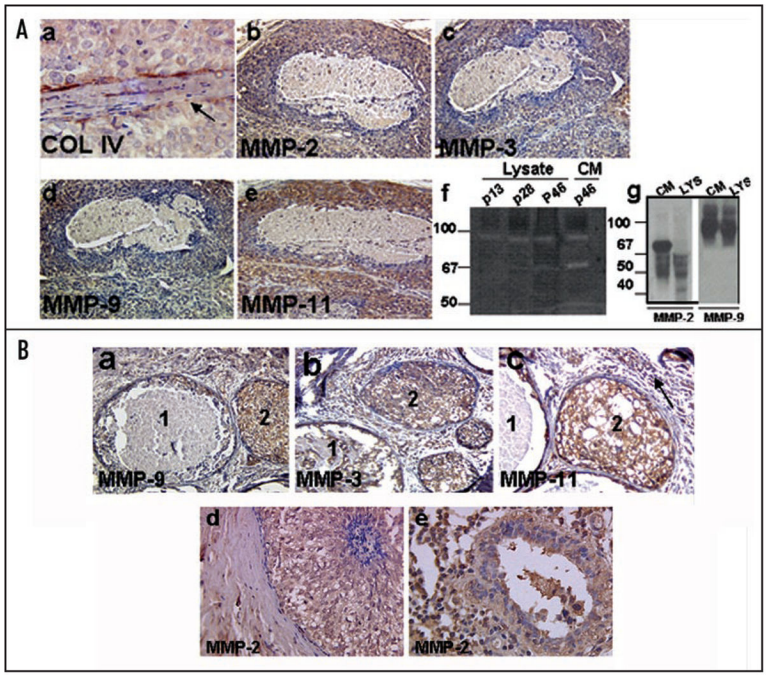

Figure 5.

(A) Immunohistochemical analysis of MMP-2, -9, -3 and -11 in day 44 MCF10DCIS.com xenografts. Note that upregulated expression of proteases is associated with breach of basement membrane as revealed by type IV collagen staining (arrow in a). Original magnification, x10 (b–e); x40 (a). Panel (f), gelatin zymography of total cell lysates or conditioned media of passages 13, 28 and 46 MCF10DCIS.com cells. Panel (g), Western blot analysis of MMP-2 and -9 in cell lysate (LYS) and conditioned media (CM) of passage 46 MCF10DCIS.com cells. (B) Immunohistochemical analysis of MMP-2, -9, -3 and -11 in clinical comedo-DCIS breast tumors. Note the presence of intense immunoreactivity to the indicated MMP in the stromal and epithelial compartments of solid (duct 2) and comedo (duct 1) DCIS lesions. Note the presence of strong reactivity to MMP-2 antibody in a duct showing very early signs of comedo formation (d) and the continued overexpression in a comedo-DCIS lesion showing lymphocytic infiltration (e). Original magnification, x10 (a and b); x20 (c and d); x40 (e).